Sains Malaysiana 55(3)(2026): 385-398
http://doi.org/10.17576/jsm-2026-5503-03

Development of Nitrogen and Phosphorous co-Doped Carbon Dots (N,P-CDs) as Fluorescent Sensor for Cu^{2+} Ions in Aquatic Environments

(Pembangunan Titik Karbon Terdop Nitrogen dan Fosforus (N,P-CDs) sebagai Sensor Pendarfluor untuk Ion Cu^{2+} dalam Persekitaran Akuatik)

KURNIAWATI AULIYAH OBBYARDI, DYAH SARSIWI HAMURWANI, ADHITASARI SURATMAN & SUHERMAN SUHERMAN*

Department of Chemistry, Faculty of Mathematics and Natural Sciences, Department of Chemistry, Faculty of Mathematics and Natural Sciences, Universitas Gadjah Mada, Yogyakarta 55281 Indonesia

Received: 16 July 2025/Accepted: 13 February 2026

ABSTRACT

A fluorescent sensor has been developed by synthesizing N,P co-doped carbon dots (N,P-CDs) through a microwave-assisted process for an early detection of Cu^{2+} in the environment. In this work, the optimization of irradiation power, irradiation time and dopant ratio of ethylenediamine and phosphoric acid as sources of N and P dopants, were studied. Further research on stability, sensitivity, selectivity, and interference to other metal ions were evaluated. FTIR analysis confirmed the success of N and P doping on the surface of CDs with the presence of characteristic bond vibrations such as N-H, C-N, and P-O. UV-Vis spectroscopy indicated the formation of carbon cores, while XRD results showed an amorphous structure. Characterization by TEM exhibited that N,P-CDs had an average size of 1.7 nm with some agglomerated parts. The N,P-CDs fluorescence sensor has a wide detection linearity range (0-0.4 ppm) with LOD and LOQ values of 0.0177 and 0.0592 ppm, respectively. Moreover, N,P-CDs effectively detected Cu^{2+} in real water samples with percentage RSD values below 5%.

Keywords: Carbon dots; copper; fluorescent sensor; microwave; nitrogen and phosphorous

ABSTRAK

Sensor pendarfluor telah dikembangkan dengan mensintesis karbon dot terdop N dan P (N,P-CDs) dengan menggunakan kaedah mikrogelombang untuk mengesan ion Cu^{2+} pada persekitaran. Dalam kajian ini, pengoptimuman daya penyinaran, waktu penyinaran serta nisbah dopan etilendiamin dan asid fosfat sebagai sumber dopan N dan P. Selain itu, kestabilan, sensitiviti, selektiviti serta pengaruh interferen daripada ion logam lain juga dinilai. Analisis FTIR hasil pendopan N dan P pada permukaan CDs dengan adanya pencirian getaran ikatan seperti N-H, C-N dan P-O. Spektroskopi UV-Vis menunjukkan pembentukan atom karbon dan hasil XRD memperlihatkan struktur amorfus. Pencirian TEM menunjukkan bahawa N,P-CDs memiliki ukuran 1.7 nm dengan beberapa bahagian mengalami aglomerasi. Sensor pendarfluor N,P-CDs memiliki kerentangan pengesanan linear yang luas (0-0.4 ppm) dengan nilai LOD dan LOQ yang diperoleh masing-masing adalah 0.0177 dan 0.0592 ppm. Selain itu, N,P-CDs secara berkesan mengesan Cu^{2+} dalam sampel air dengan nilai peratusan RSD yang kurang daripada 5%.

Kata kunci: Karbon dot; kuprum; mikro gelombang; nitrogen dan fosforus; sensor pendarfluor

INTRODUCTION

The rapid growth of industry and population has driven economic development, but it has also caused serious environmental issues, particularly water pollution. Water quality is influenced by both anthropogenic and natural sources of contamination (Suaad 2021). Among various pollutants, heavy metals are of major concern due to their non-biodegradable nature and tendency to bioaccumulate in living organisms. One such metal, copper ions (Cu^{2+}), is widely used in industries such as metallurgy, metal plating, batteries, and chemicals, and is frequently detected in industrial wastewater. This contamination poses a threat to ecosystems, hinders plant growth, and endangers human health (Algethami & Abdelhamid 2024). According to Indonesia's Ministry of Health Regulation No. 2 of 2023, which refers to Government Regulation No. 22 of 2021, the maximum permissible Cu^{2+} concentration in class I water is 0.2 mg/L.

Various analytical techniques, including AAS, ICP-OES, ICP-MS, HPLC, and electrochemical methods, have been employed to detect Cu^{2+} ions (Brito et al. 2025; Erdiwansyah et al. 2025; Wang et al. 2022). However, these

methods require sophisticated instruments, are expensive, and time-consuming, limiting their suitability for rapid field monitoring. As an alternative, fluorescence-based optical sensors have gained attention due to their practicality, sensitivity, and cost-effectiveness (Shi et al. 2023). Carbon dots (CDs) are promising fluorescent materials due to their low synthesis cost, good biocompatibility, and ease of surface functionalization (Sahu & Khan 2020). CDs can be synthesized through top-down and bottom-up methods, are known for uniform characteristics and enhanced fluorescence intensity. The microwave-based bottom-up synthesis, in particular, offers advantages like cost-effectiveness, rapid heating, and high product purity (Tabaraki & Abdi 2020). Compared to conventional synthesis methods, including hydrothermal, solvothermal, and pyrolysis, microwave irradiation offers several distinct advantages in the synthesis of CDs. Microwave heating is a volumetric process that occurs through the direct interaction of electromagnetic radiation with polar molecules and ions in the reaction medium, enabling rapid, uniform, and energy-efficient heating. In contrast, conventional heating relies on heat transfer through conduction and convection, which generally requires longer processing times and often results in non-uniform temperature distribution (Al Farsi et al. 2022).

Despite their extraordinary potential, undoped CDs composed only of carbon and oxygen often exhibit low fluorescence efficiency due to non-radiative recombination caused by epoxy and carboxyl groups on their surface (Fu et al. 2024). To overcome this limitation, heteroatom doping both with metal and non-metal elements has been employed. Non-metal doping using elements such as nitrogen (N), sulfur (S), phosphorus (P), and boron (B) is considered safer and more effective. Among these, N and P doping are the most commonly applied due to their synergistic effects in enhancing both luminescence and conductivity (Fu et al. 2024; Park et al. 2015). This is due to the size of N and P atoms being similar to carbon atoms, allowing them to easily enter the structure of CDs. The five valence electrons of N dopants can facilitate electronic transitions from the ground state to the excited state, this transition results in a change in the band gap, significantly increasing the fluorescence intensity of CDs (Yan et al. 2019). P dopants have a much larger atomic radius than C atoms, making P dopants more prone to electronic transitions than C atoms. Due to their ability to act as n-type donors and form substitution defects in sp^3 diamond thin films, doping CDs with P elements can improve their electronic properties (Zhou et al. 2017).

In previous study conducted by Kamal et al. (2024), P,N-doped carbon quantum dots (P,N-CDs) were synthesized via a 180 s microwave method using EDTA and diammonium hydrogen phosphate as precursors. The resulting NP@CQDs exhibited strong blue fluorescence at 420 nm (excited at 360 nm) and demonstrated high sensitivity and precision in detecting glutathione (GSH) within 0.5-10 µg/mL. In this study, a fluorescent sensor based on N,P-doped carbon dots (N,P-CDs) was developed using the microwave synthesis method. Citric acid, ethylenediamine, and phosphoric acid were employed as precursors. The goal of this research was to create a rapid, sensitive, selective, and affordable method for detecting Cu^{2+} ions in aquatic environments. This approach is expected to provide a simpler and more efficient alternative to conventional instrumental techniques used for analyzing heavy metals in water.

MATERIALS AND METHODS

MATERIALS

The precursors used for synthesizing N,P-CDs were citric acid monohydrate ($C_6H_8O_7 \cdot H_2O$), ethylenediamine ($C_2H_4(NH_2)_2$), 85% phosphoric acid (H_3PO_4), and distilled water (aquabidest). The chemicals used for sensitivity and selectivity tests included NaOH, $Cd(CH_3COO)_2$, $CuCl_2 \cdot 2H_2O$, $MgCl_2 \cdot 6H_2O$, $CaCl_2 \cdot 2H_2O$, $MnCl_2$, $NiCl_2 \cdot 6H_2O$, $AlCl_3 \cdot 6H_2O$, $BaCl_2 \cdot 2H_2O$, KCl, and $ZnCl_2$, all purchased from Merck with pro analysis grade. The environmental water samples used in this study were tap water (PDAM), well water, Code River water, and Manunggal River water.

INSTRUMENTATIONS

Laboratory equipment was glassware, a digital balance (Mettler Toledo ME 204), micropipette (Eppendorf Research Plus), a microwave (Samsung ME371K), and pH meter. The characterization instruments used were a UV-Vis spectrophotometer (Thermo Scientific GENESYS 150), Fourier-transform infrared spectroscopy (FTIR, Shimadzu IPRPrestige-21), a Spectrofluorometer (RF-6000 Shimadzu), an X-ray diffractometer (XRD, Bruker AXS D8 Advance Eco), and a Transmission electron microscope (TEM, JEOL JEM-1400, Japan).

SYNTHESIS OF N,P-CDs

N,P-CDs were synthesized using a microwave-assisted method with 100 mg of citric acid, 55.6 µL of ethylenediamine, and 29.6 µL of phosphoric acid as precursors. The mixture was irradiated at various microwave power levels (100, 180, 300, 450, 600, and 800 W) for 1.5 min to optimize power, with the power range selected based on the display of the microwave device used. Irradiation was performed in stages. The irradiation time of 1.5 min was determined as the optimum condition based on the optimization of the synthesis time (1, 1.5, 2, 2.5, 3, and 3.5 min). During optimization, the irradiation time and power were alternately kept constant, and all treatments were carried out with the same amount of precursor and reaction volume. The resulting N, P-CDs were dissolved in 10 mL deionized water and their fluorescence intensities were measured (λ_{ex} 200-600 nm) to determine optimal conditions. Further optimization

involved varying the ratio of phosphoric acid and ethylenediamine (0, 12.5, 25, 50, 75, and 100%) under the selected irradiation parameters. The optimized N, P-CDs were characterized by UV-Vis, FTIR, XRD, and TEM analysis.

STABILITY OF N,P-CDs

The stability of N,P-CDs was evaluated under varying conditions of pH, storage period, and UV exposure. pH stability was tested by adjusting the solution pH from 2 to 9. For UV exposure testing, the N,P-CDs solution was irradiated with UV light for 0-90 min. Storage stability was assessed over 21 days at room temperature and ±4 °C in sealed containers. Fluorescence intensity was measured at the maximum wavelength (350 nm) for all conditions.

OPTIMIZATION OF Cu^{2+} ION ANALYSIS CONDITIONS USING N,P-CDs

The analysis conditions for Cu^{2+} ions using N,P-CDs were evaluated based on variations in analyte pH and response time of the analyte toward the N,P-CD fluorescent nanosensor. To determine the optimal quenching effect, the interaction stability between N, P-CDs, and the target metal ion Cu^{2+} was assessed across a range of pH values (2-9), fluorescence intensity was then measured using a spectrofluorometer with an λ_{ex} of 350 nm.

DETECTION OF Cu^{2+}

The detection of Cu^{2+} ions was performed by investigating the effect of various concentrations of Cu^{2+} (0-32 ppm) on the fluorescence intensity of N,P-CD. The concentration range selected to ensure that the sensor response remained measurable at both low and high concentrations. Each measurement was repeated three times for each Cu^{2+} concentration. Fluorescence intensity was then measured using a spectrofluorometer with an λ_{ex} of 350 nm.

SENSITIVITY OF N,P-CDs FOR Cu^{2+} DETECTION

Sensitivity testing was conducted to evaluate the ability of N,P-CDs to detect Cu^{2+} ions. Various Cu^{2+} concentrations (0-0.4 ppm) were prepared, and 4 mL of each solution was mixed with 1 mL of N,P-CDs. Fluorescence intensity was measured at an excitation wavelength of 350 nm, with all measurements performed in triplicate. A calibration curve was constructed by plotting %quenching $[(F_0–F)/F_0 \times 100]$ against Cu^{2+} concentration, where F_0 and F represent the fluorescence intensity before and after Cu^{2+} addition, respectively. The limit of detection (LOD) and limit of quantification (LOQ) were calculated using the formulas:

$$\mathrm{LOD} = \frac{3\ x\ Sr}{b} \quad (1)$$

$$\mathrm{LOQ} = \frac{10\ x\ Sr}{b} \quad (2)$$

where *Sr* represent the standard deviation of the blank signal and *b* refers to the slope of the calibration curve.

SELECTIVITY AND INTERFERENCE OF N,P-CDs TO OTHER METAL IONS

The selectivity of N,P-CDs was evaluated by measuring their fluorescence intensity in the presence of various metal ions, including Cd^{2+}, Na^{+}, Mn^{2+}, Ni^{2+}, Ba^{2+}, Ca^{2+}, Mg^{2+}, Al^{3+}, and Zn^{2+}. Selectivity testing was conducted by mixing 1 mL of N,P-CDs solution with 4 mL of each 200 ppm metal ion solution, followed by fluorescence measurement at an excitation wavelength (λ_{ex}) of 350 nm. For the interference test, 1 mL of N,P-CDs was added to a mixture of 4 mL Cu^{2+} solution (200 ppm) and 2 mL of each interfering cation solution (200 ppm). The mixtures were analyzed using a spectrofluorometer at λ_{ex} 350 nm to evaluate whether the presence of other metal ions significantly affected the detection of Cu^{2+}.

APPLICATION OF N,P-CDs FOR Cu^{2+} IN REAL SAMPLE

The application of N,P-CDs was evaluated by testing them on various water samples, including PDAM (municipal tap water), well water, Manunggal River water, and Code River water in Yogyakarta. Each water sample (4 mL) was mixed with 1 mL of N, P-CDs solution, which had been adjusted to a pH of 6. The mixtures were then analyzed using a spectrofluorometer with an λ_{ex} of 350 nm. Each test was performed in triplicate.

RESULTS AND DISCUSSION

OPTIMIZATION OF IRRADIATION POWER FOR SYNTHESIS OF N,P-CDs

N,P-CDs were successfully synthesized using the microwave-assisted method, which offers several advantages over conventional methods, such as a simpler process, shorter reaction time, and higher equipment efficiency (Al Farsi et al. 2022). Based on Figure 1(a), fluorescence measurements showed that intensity increased with power up to 450 W and then decreased, indicating that 450 W was the optimal condition for producing N,P-CDs with the highest fluorescence intensity. This increase is associated with the enhanced formation of surface functional groups at 450 W, which improves light absorption and fluorescence emission (Sutanto et al. 2020). In contrast, excessive power (>450 W) can lead to over-carbonization, particle aggregation, and a reduction in surface functional groups, ultimately resulting in decreased fluorescence intensity (Alkian, Sutanto & Hadiyanto 2022).

Based on Figure 1(b), fluorescence analysis showed that intensity increased with irradiation time, peaking at 1.5 min, and then gradually declined from 2 to 3.5 min. The optimal irradiation time of 1.5 min corresponds to the complete formation of a passivated sp^2 carbon core, which enhances surface fluorescence due to increased formation of fluorophore polymer chains (Zhang et al. 2016). While extended irradiation promotes polymerization and surface passivation, excessive heating beyond the optimum can damage the surface structure, causing a decrease in fluorescence a 'turn-off' effect. Conversely, insufficient irradiation results in incomplete carbonization, also reducing fluorescence efficiency (Wang et al. 2022).

OPTIMIZATION OF N AND P DOPANT PERCENTAGES IN N,P-CDs

Optimization N,P-CDs was conducted in two stages, first by varying the amount of ethylenediamine, followed by the addition of phosphoric acid. Doping with heteroatoms like N and P alter the electronic structure of CDs, improving their fluorescence performance (Kamal et al. 2024). For nitrogen and phosphor doping, it was tested at ratios 0%, 12.5%, 25%, 50%, 75%, and 100%.

Based on Figure 2(a), fluorescence intensity increased with doping percentage and reached its peak at 25%, then declined at higher ratios. This enhancement is attributed to nitrogen's ability to integrate into the carbon framework and act as an electron donor, modifying the internal electronic environment and enhancing fluorescence (Lin et al. 2019). Similarly, based on Figure 2(b), phosphorus doping using phosphoric acid showed the highest fluorescence intensity at a 25% ratio. Phosphorus atoms, being larger than carbon, can fill defect sites and act as n-type dopants, effectively tuning the structural and optical properties of the CDs (Gong et al. 2017).

The fluorescence intensity of N,P-CDs was measured at excitation wavelengths from 300 to 400 nm (Figure 3). The intensity increased with excitation wavelength, peaking at 350 nm, indicating this as the optimal excitation wavelength that produces the highest emission due to efficient electron excitation. Beyond 350 nm, fluorescence intensity decreased, suggesting reduced efficiency in electron transition back to the ground state, leading to lower light emission (Zhou et al. 2017). Excitation at 350 nm produced a maximum emission peak at 460 nm, corresponding to blue light emission. As the excitation wavelength increased further, redshift in the emission spectrum occurred, along with reduced intensity and narrower peak width. This redshift is attributed to variations in particle size and differences in surface functional groups among the N,P-CDs (Atchudan et al. 2020).

CHARACTERIZATION OF N,P-CDs

The structure and characterization of N,P-CDs have been analyzed using UV-Vis spectrophotometer, FTIR, XRD, and TEM. Figure 4 illustrates the absorption, excitation, and emission spectra of the N, P-CDs material, indicating significant absorption and excitation in the UV to visible light range. The absorption spectrum shows two prominent peaks at wavelengths of 250 nm and 350 nm. The peak at 250 nm is attributed to π–π^* electronic transitions of the aromatic sp^2 domains, while the peak at 350 nm corresponds to n–π^* transitions, suggesting the presence of functional groups such as C=O or C=N. These features confirm the successful formation of N, P-CDs, characterized by aromatic carbon cores along with carboxylate and amide surface groups (Huang et al. 2018). The excitation spectrum exhibits a maximum at 350 nm, indicating the optimum wavelength for exciting material to achieve efficient fluorescence emission. Meanwhile, the emission spectrum displays a peak at 450 nm, representing the maximum emission wavelength. These spectral characteristics demonstrate strong photoluminescent properties attributed by N,P-CDs, with active electron transitions and surface structures that supported intense and stable light emission.

FTIR analysis of N,P-CDs confirmed the presence of various functional groups, as shown in Figure 5. In Figure 5(a), the FTIR spectra of citric acid show absorption bands at 1728 and 1173 cm^{-1}, which are related to C=O and C–O stretching vibrations, respectively, as well as a broad band at 3372 cm^{-1}, which indicates O–H stretching vibrations. Ethylenediamine and phosphoric acid, which act as nitrogen and phosphorus passivators in CDs, exhibit FTIR spectra as shown in Figure 5(b) and 5(c). Ethylenediamine displays a broad band at 3356 cm^{-1} and a sharp band at 1597 cm^{-1} associated with N–H stretching and bending vibrations, respectively, while phosphoric acid shows bands at 1003 and 895 cm^{-1} associated with P–O stretching and P–OH bending vibrations (Yang et al. 2019; Zhang et al. 2019).

FTIR spectra of N,P-CDs (Figure 5(d)) show a broad band at 3379 cm^{-1} and a peak at 1705 cm^{-1}, indicating the presence of carboxyl groups. The peak at 1651 cm^{-1} indicates the formation of amide bonds, while the band at 1096 cm^{-1} is related to C–O stretching vibrations. The success of nitrogen doping is indicated by the appearance of bands at 3248, 1551, and 1404 cm^{-1}, which are related to N–H stretching, N–H bending, and C–N stretching vibrations, respectively. Meanwhile, phosphorus doping is confirmed by bands at 1296, 1057, and 949 cm^{-1} associated with P=O, P–O–C, and P–H bending vibrations, as well as a band at 555 cm^{-1} associated with phosphate group (PO_4^{3-}) vibrations (Huang et al. 2018; Yang et al. 2019). The presence of these peaks confirms that nitrogen and phosphorus atoms have been successfully integrated into the structure of N,P-CDs.

The diffractogram of N,P-CDs shown in Figure 6 indicates that the synthesized N,P-CDs contain carbon atoms arranged in an asymmetric and amorphous crystalline pattern due to the presence of surface functional groups. The presence of a graphene-like structure in the core of the

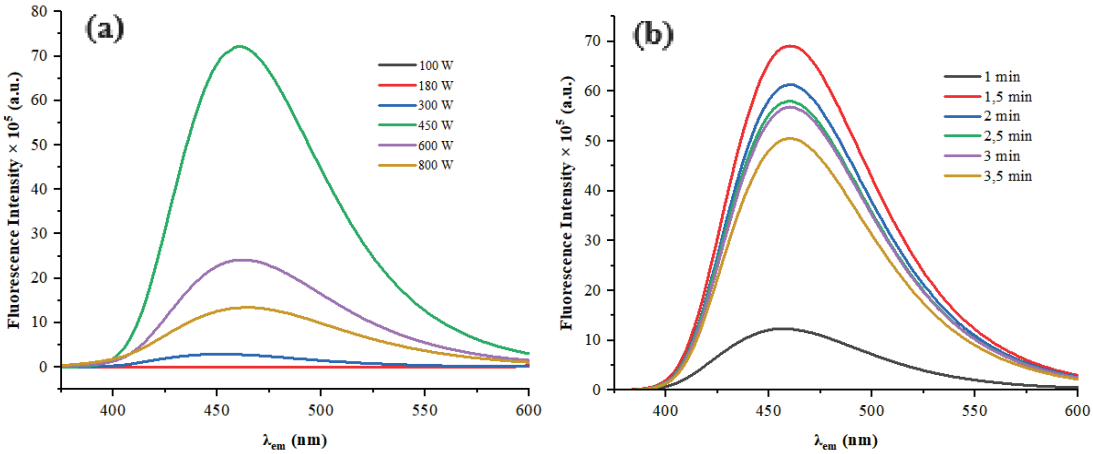

FIGURE 1. Fluorescence spectra of N,P-CDs with varying (a) irradiaton power and (b) irradiation time

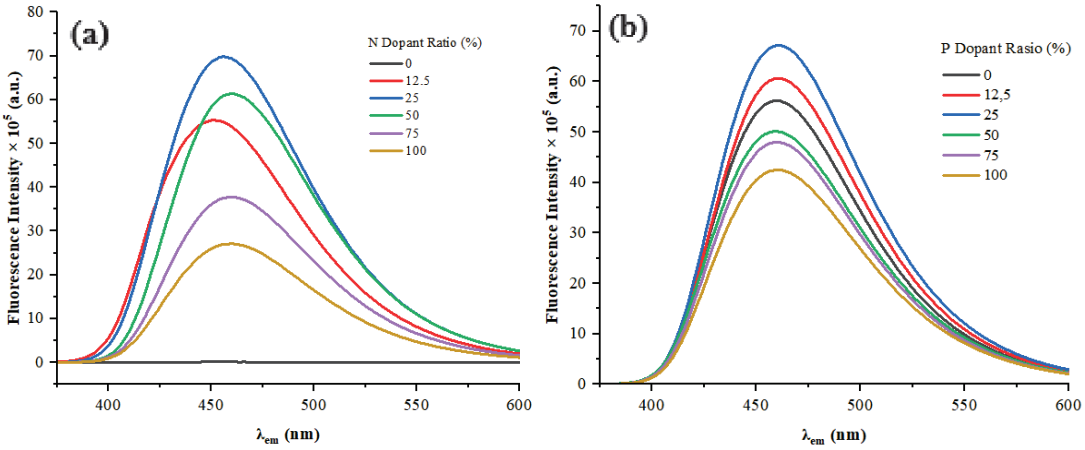

FIGURE 2. (a) Fluorescence spectra of N,P-CDs with varying N dopant ratio and (b) P dopant ratio

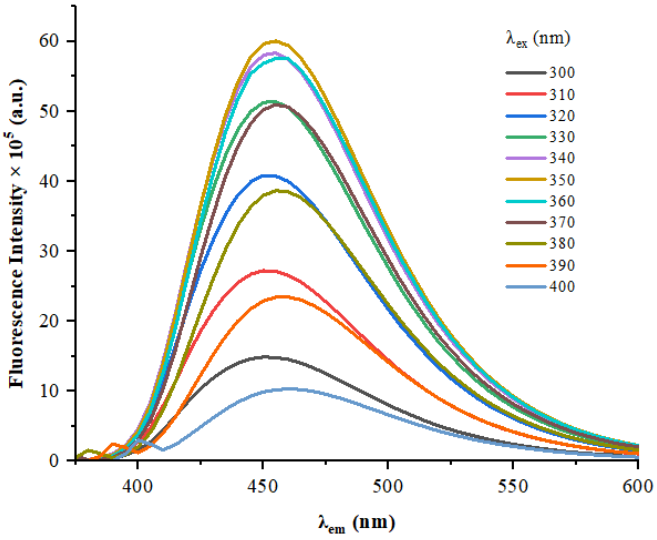

FIGURE 3. Photoluminescent emission spectra of N,P-CDs
at different excitation wavelengths

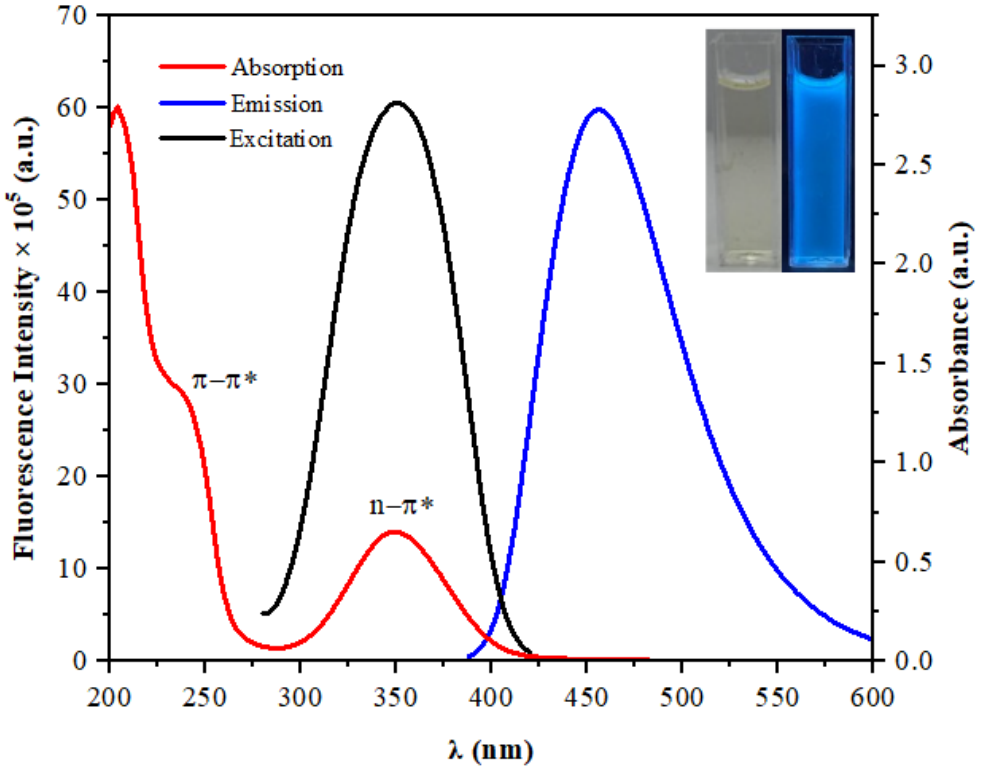

FIGURE 4. The absorption, excitation, and emission spectra of the optimal N, P-CDs

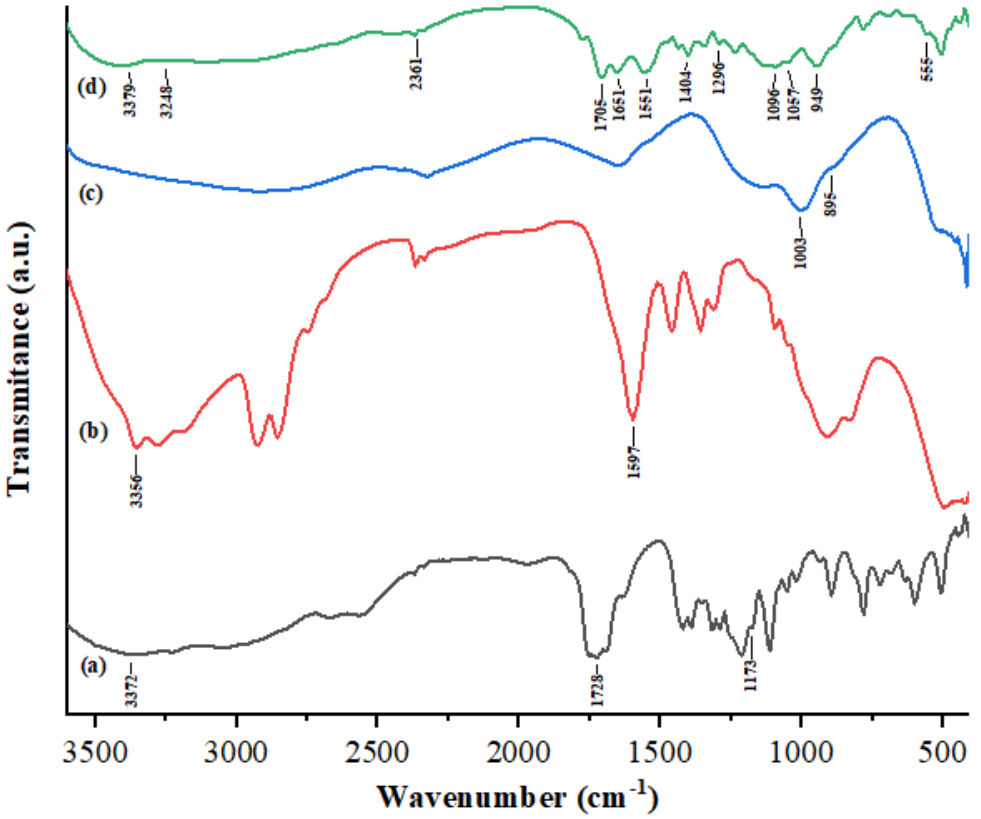

FIGURE 5. The FT-IR spectra of (a) citric acid, (b) ethylenediamine, (c) phosphoric acid, and (d) N,P-CDs

N,P-CDs is confirmed by the appearance of several peaks at 2θ = 21.2°, 26.5°, and 35.8°, corresponding to the (002), (102), and (103) crystal planes. Among these, the first two peaks refer to graphite (sp^2) structures, while the last peak indicates the presence of diamond like (sp^3) carbon a characteristic consistent with the fundamental properties of carbon (Atchudan et al. 2020).

The morphology and size distribution of the synthesized N,P-CDs were analyzed using TEM (Figure 7). The particles exhibited quasi-spherical shapes and were generally well-dispersed in water, although some aggregation was observed due to the extremely small particle sizes and high particle density, which led to nanoscale interparticle distances (Kaur et al. 2020). Size distribution analysis using ImageJ showed that the particles ranged from 1 to 2.4 nm, with an average diameter of 1.7 nm. The uniformity in particle size is attributed to the microwave-assisted synthesis, which promotes more consistent carbonization (Lin et al. 2019).

STABILITY OF N,P-CDs

The Stability of N,P-CDs in Different pH Conditions

The photoluminescence stability of N,P-CDs was tested across a pH range of 2-9. Based on Figure 8(a), fluorescence intensity increased from pH 2 to 4, peaked at pH 6, and then slightly decreased up to pH 9. Despite the decline, intensity remained relatively stable between pH 6 and 9, indicating good photostability under mildly acidic to basic conditions. This behavior is influenced by the protonation and deprotonation of surface functional groups such as $–NH_2$, –OH, –COOH, and $–PO_4$ (Diana et al. 2022). At low pH (e.g., pH 2), strong protonation leads to surface aggregation and fluorescence quenching (Liu et al. 2021; Shen et al. 2021). In contrast, at higher pH, deprotonation enhances stability, especially of –COOH, –OH, and $–PO_4$ groups, while $–NH_2$ becomes less active. Overall, these results confirm that N,P-CDs exhibit favorable fluorescence properties and structural stability within the pH range of 6 to 9, making them well-suited for sensing applications in diverse environmental conditions.

Photostability is a key parameter in evaluating the structural integrity and fluorescence performance of fluorescent materials under light exposure, including phenomena such as photobleaching or photo enhancement (Tan et al. 2014). Carbon dots are known for their excellent photostability, and this study assessed the UV stability of N,P-CDs by exposing them to 15W UV light for up to 90 min at 15-min intervals. As shown in Figure 8(b), the fluorescence intensity of N,P-CDs exhibited no significant decrease throughout the exposure period. These results indicate that the fluorophore content of N,P-CDs remains resistant to photodegradation, confirming their stable photoluminescence under prolonged UV irradiation. Therefore, N,P-CDs demonstrate strong photostability and are well-suited for applications requiring exposure to UV light.

The photostability of N,P-CDs was investigated under two storage conditions: room temperature (RT) and cold storage at ±4 °C, as shown in Figure 8(c). Fluorescence measurements over 21 days showed that samples stored at ±4 °C retained higher and more stable fluorescence intensity than those at RT. At room temperature, a gradual decline in fluorescence was observed, especially after day 5, likely due to surface degradation or oxidation of functional groups involved in emission efficiency (Liu et al. 2021; Shen et al. 2021). In contrast, N,P-CDs stored at ±4 °C showed stable fluorescence, with slight increases on days 5 and 15, indicating good structural preservation and photostability. These results suggest that N,P-CDs remain stable for at least 15 days under cold storage. Their excellent stability is attributed to their small particle size, high graphitic nitrogen content, and reactive surface groups, which help maintain emission performance (Issa et al. 2019).

Optimization of Cu^{2+} Ion Analysis Conditions with N,P-CDs

Cu^{2+} detection using N,P-CDs was optimized by evaluating the effect of solution pH (2-9), with the N,P-CDs pre-adjusted to pH 6 based on prior stability results. The degree of fluorescence quenching was used to assess the interaction efficiency between Cu^{2+} and the surface of N,P-CDs. As shown in Figure 9, the fluorescence intensity of N,P-CDs without Cu^{2+} increased from pH 2 to 3 and remained stable between pH 3 and 9. This suggests that the strong protonation of surface groups, such as –COOH and $–NH_2$, at pH 2 suppresses fluorescence, while deprotonation at higher pH levels stabilizes the surface and enhances emission.

Following the addition of Cu^{2+}, fluorescence intensity significantly decreased across all pH levels, with the most pronounced quenching observed at pH 5, indicating strong coordination between Cu^{2+} and surface groups on N,P-CDs (Liu et al. 2021). Above pH 7, a further decline in intensity was observed, likely due to the formation of insoluble $Cu(OH)_2$, which limits the availability of free Cu^{2+} for interaction. These findings demonstrate that solution pH significantly influences Cu^{2+}-CDs interactions, and that pH 6 is the optimal condition for sensitive and efficient Cu^{2+} detection using N,P-CDs based sensor.

Effect of Cu^{2+} Concentration on N,P-CDs Fluorescence Intensity and Their Sensitivity

The synthesized N,P-CDs were successfully applied for Cu^{2+} detection in water through a fluorescence quenching mechanism. The sensitivity of N,P-CDs in detecting Cu^{2+} was evaluated by monitoring the decrease in fluorescence intensity (quenching) as different concentrations of Cu^{2+} were added to the N,P-CDs solution. As shown in Figure 10(a), the fluorescence intensity decreased significantly with increasing Cu^{2+} concentration in the range of 0 to 32 ppm, indicating an effective quenching response (Zhang et al. 2022).

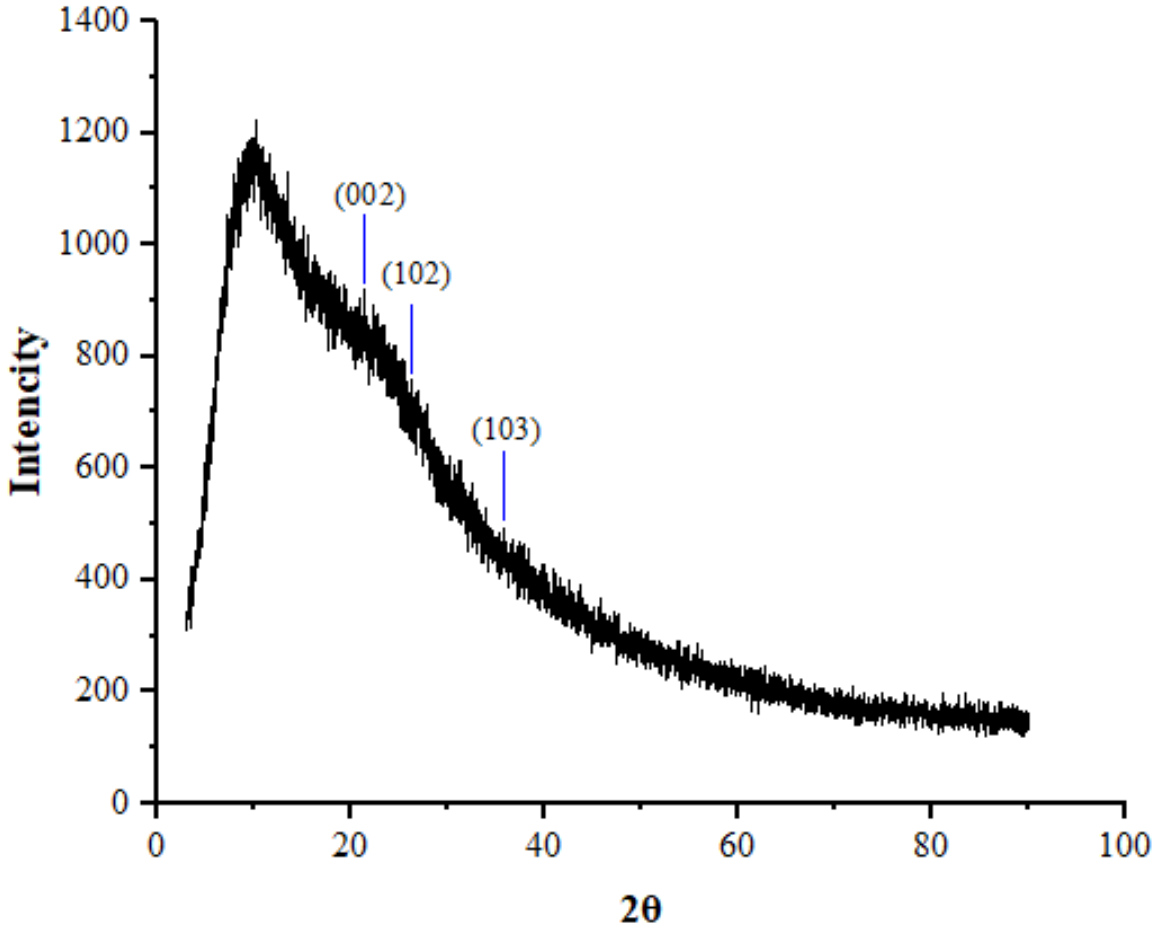

FIGURE 6. Diffractogram of N,P-CDs

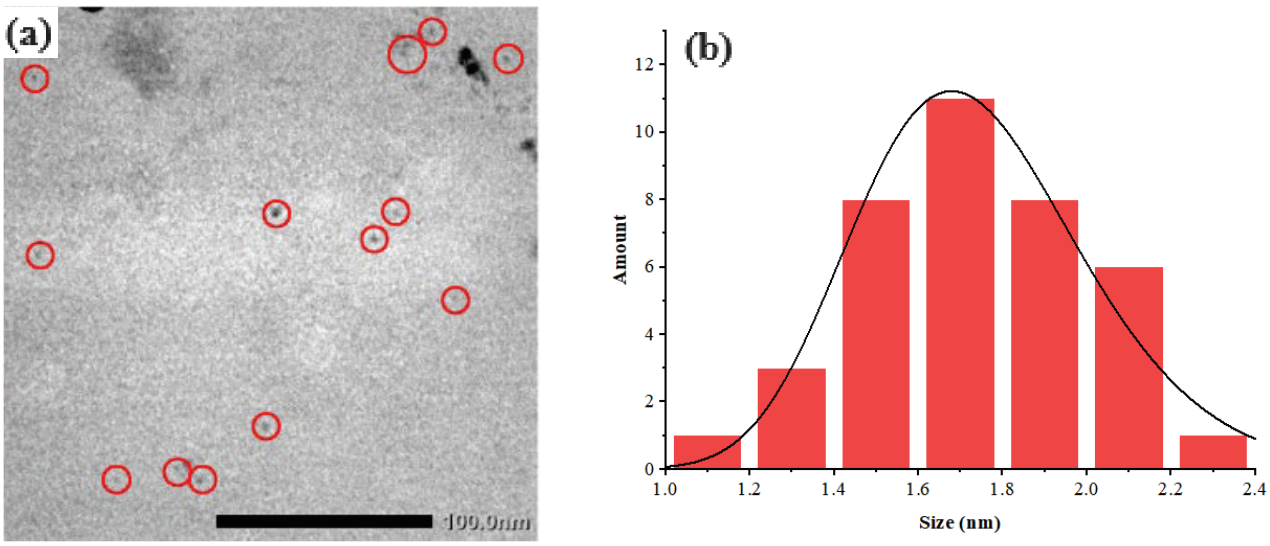

FIGURE 7. (a) N,P-CDs TEM image and (b) size distribution

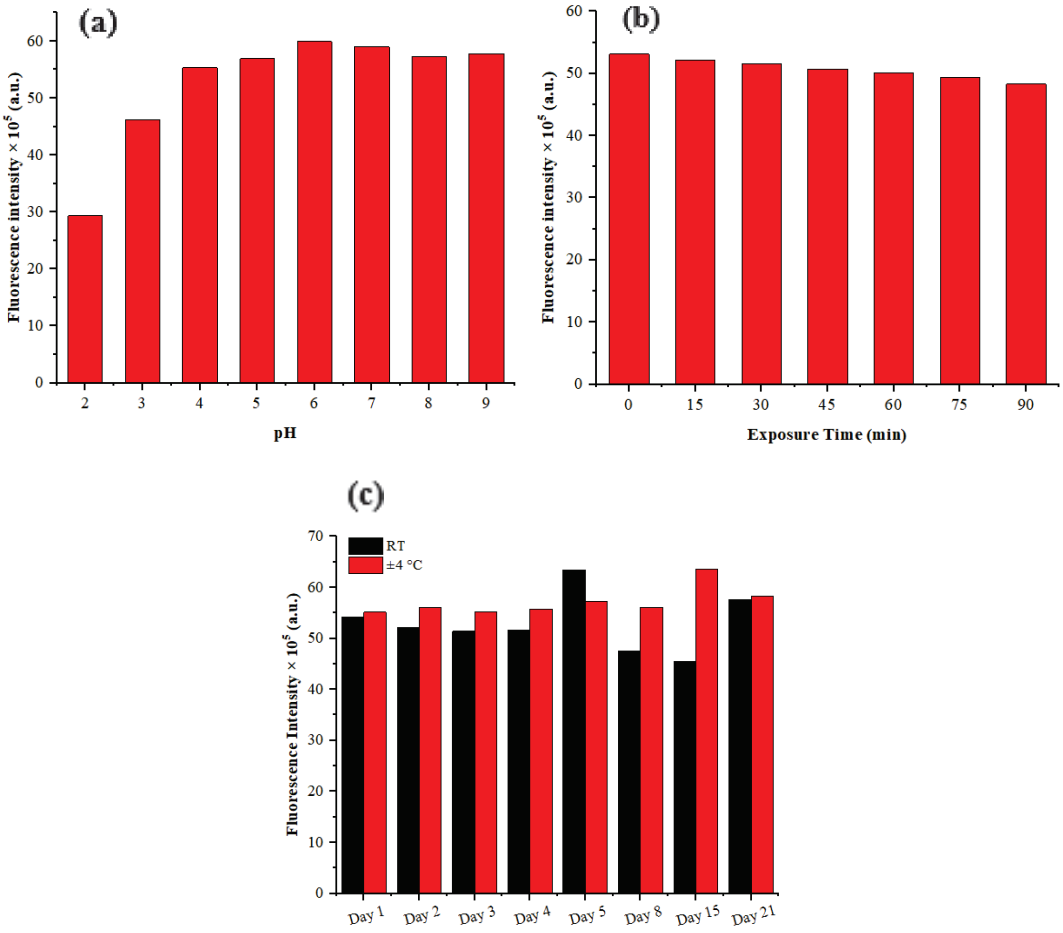

FIGURE 8. The stability of N,P-CDs in (a) different pH conditions (b) UV exposure, and (c) storage period

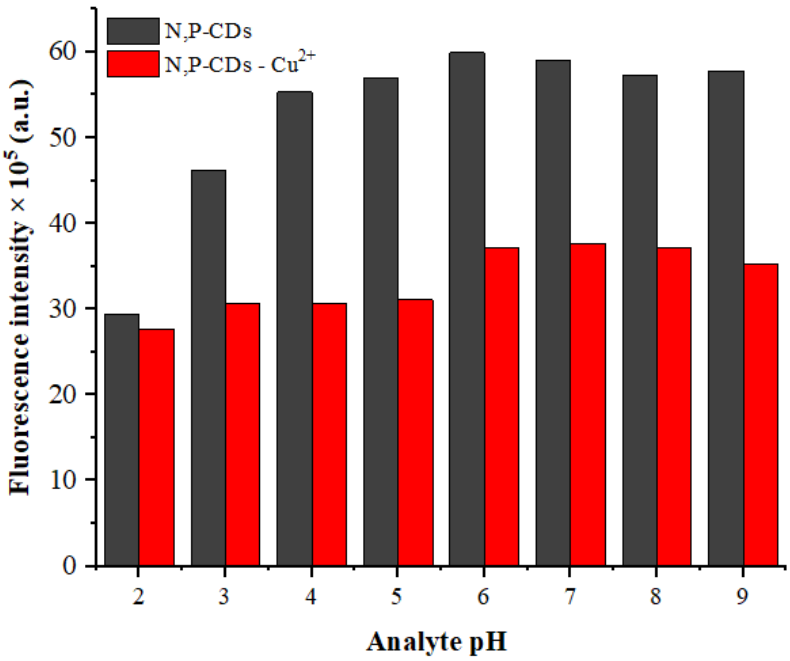

FIGURE 9. Effect of analyte pH on N,P-CDs after Cu^{2+} addition

A more detailed analysis was conducted in the lower concentration range of 0 to 0.4 ppm, as presented in Figure 10(b). The inset graph shows a strong linear correlation between the percentage of fluorescence quenching and Cu^{2+} concentration, with a coefficient of determination (R^2) of 0.9985. This excellent linearity confirms that N,P-CDs can provide reliable quantitative detection within this range. The LOD was determined to be 0.0177 ppm, this value demonstrates that N,P-CDs possess high sensitivity toward Cu^{2+} ions and can detect trace amounts effectively. Importantly, this LoD is significantly lower than the maximum allowable Cu^{2+} concentration set by the World Health Organization (WHO) and Indonesia's Ministry of Health Regulation No. 2 of 2023, which is 0.2 ppm for Class I drinking water. In addition to LoD, the LOQ which represents the lowest concentration that can be measured quantitatively with acceptable accuracy and precision. The resulting LoQ value of 0.0592 ppm further supports the reliability of N,P-CDs as a quantitative sensor for Cu^{2+}. These findings confirm that N,P-CDs exhibit excellent analytical performance in terms of both sensitivity and linear detection range, making them a promising fluorescent nanosensor for monitoring copper ion contamination in real environmental samples.

SELECTIVITY AND INTERFERENCE TEST OF N,P-CDs TO OTHER METAL ION

Selectivity and interference tests were conducted to evaluate the ability of N,P-CDs to detect Cu^{2+} ions in the presence of various other metal cations, including Na^+, K^+, Ca^{2+}, Mg^{2+}, Al^{3+}, Cd^{2+}, Zn^{2+}, Ni^{2+}, and Mn^{2+}. The selectivity and interference assessment were performed at pH 6, with each cation tested at a concentration of 200 ppm. Based on Figure 11, only Cu^{2+} ions significantly reduced the fluorescence intensity of N,P-CDs, with a quenching efficiency of 41.8%, while the other cations showed negligible effects on the fluorescence signal. Quenching by Cu^{2+} occurs through a photoinduced electron transfer (PET) mechanism, namely the transfer of excited electrons from N,P-CDs to partially filled Cu^{2+} orbitals, thereby inhibiting fluorescence emission. In contrast, other metal ions do not cause a significant decrease in fluorescence because they have weaker coordination interactions with N,P-CDs, or do not provide suitable empty orbitals to accept electrons. Therefore, only Cu^{2+} acts as an effective electron acceptor, selectively quenching fluorescence (Lou et al. 2025).

Furthermore, when Cu^{2+} ions were tested in a mixed-ion matrix containing other metal cations, the fluorescence of N,P-CDs still exhibited significant quenching. This result indicates that the presence of different ions does not interfere with or inhibit the interaction between N,P-CDs and Cu^{2+}, confirming the high selectivity of the nanosensor toward Cu^{2+} ions.

The high selectivity of N,P-CDs toward Cu^{2+} is attributed to the PET mechanism, as presented in Figure 12. In this process, surface functional groups on N,P-CDs (–OH, $–NH_2$, –COOH) act as electron donors. When excited by light, electrons transition from the HOMO to the LUMO, but instead of returning to the ground state and emitting fluorescence, they are transferred to the empty 3d orbitals of Cu^{2+} ions, which act as electron acceptors. This transfer forms a coordination complex between N,P-CDs and Cu^{2+}, disrupting the radiative recombination process that typically produces fluorescence. As a result, fluorescence intensity significantly decreases. The strong binding affinity between Cu^{2+} and the surface groups, combined with the efficient PET mechanism, explains the excellent selectivity of N,P-CDs in detecting Cu^{2+} even in the presence of other metal ions (Liu et al. 2018).

APPLICATION OF N,P-CDs TO DETECT THE PRESENCE OF Cu^{2+} IN REAL SAMPLES

The fluorescent sensor N,P-CDs was successfully applied to detect Cu^{2+} ions in various environmental water samples,

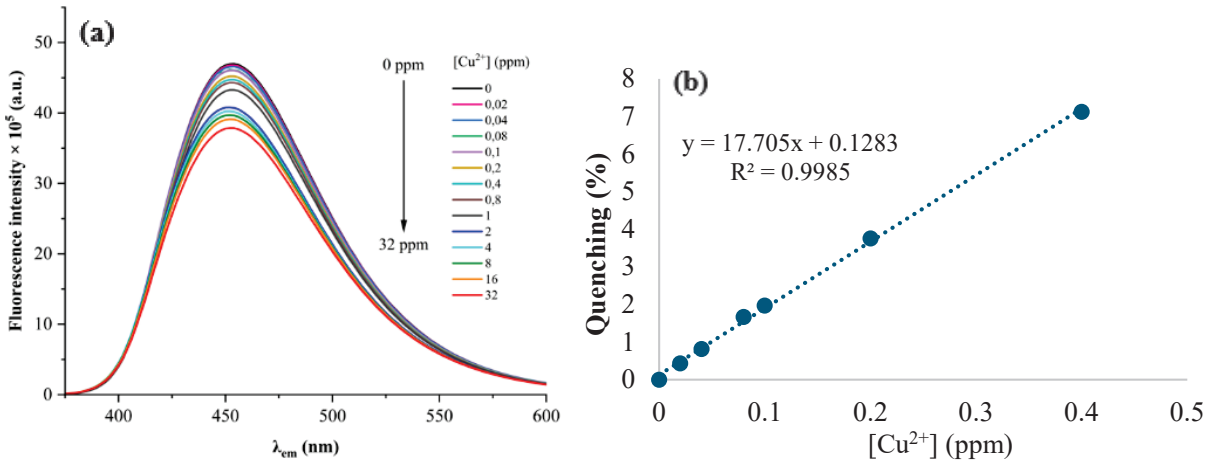

FIGURE 10. (a) Fluorescence spectra of N,P-CDs after addition of Cu^{2+} with various concentrations and (b) Linear plot for fluorescence quenching of N,P-CDs after addition of Cu^{2+} at various concentrations

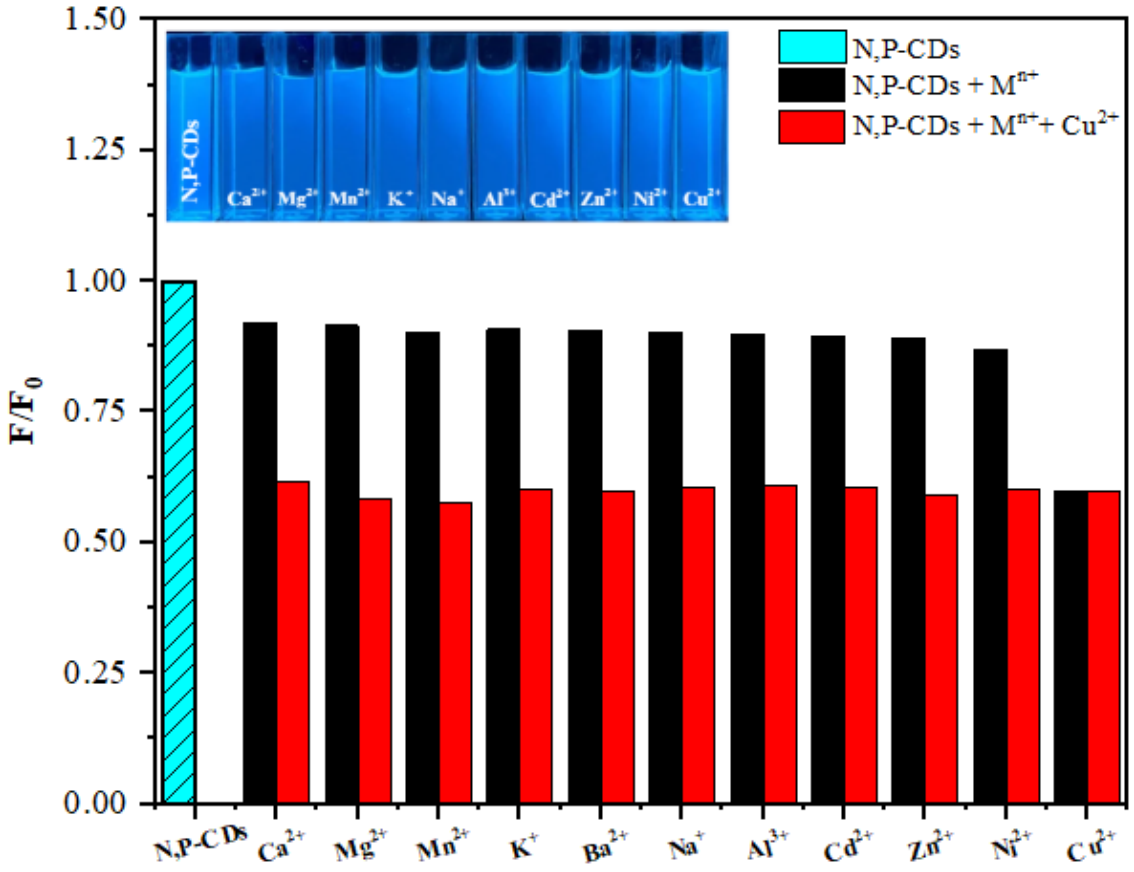

FIGURE 11. Selectivity and interference of N,P-CDs towards various cations

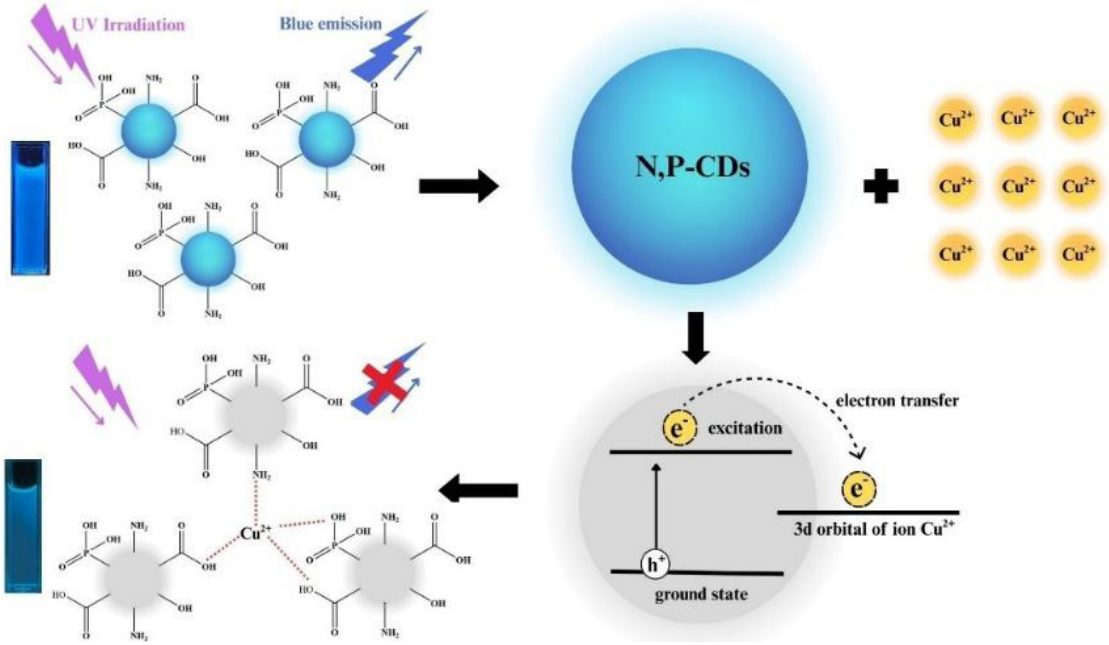

FIGURE 12. N,P-CDs interaction with Cu^{2+}

including municipal tap water (PDAM), well water, and water from the Code and Manunggal Rivers. The sensor demonstrated good sensitivity and selectivity toward Cu^{2+}. Each measurement was performed in triplicate, and the Relative Standard Deviation (RSD) was used to evaluate the accuracy and precision of the results. Figure 13 indicated that increasing of Cu^{2+} concentration in the samples corresponded with a greater decrease in fluorescence intensity.

The fluorescence intensities from the four samples were analyzed using the calibration curve to determine the Cu^{2+} concentrations. Based on Table 1, the calculated concentrations were, 0.50 ppm (PDAM water), 1.06 ppm (well water), 0.99 ppm (Code River), and 1.03 ppm (Manunggal River). All these values exceed the maximum limit set by Indonesia's Ministry of Health Regulation No. 2 of 2023, which specifies a threshold of 0.2 ppm for Cu^{2+} in drinking water, indicating significant contamination. Moreover, the method demonstrated high precision with %RSD values below 5%, confirming the accuracy and reliability of the N,P-CDs sensor for real sample analysis. Overall, this study demonstrates that N,P-CDs have strong potential as a low-cost, simple, selective, and sensitive fluorescent sensor for monitoring Cu^{2+} in aquatic environments.

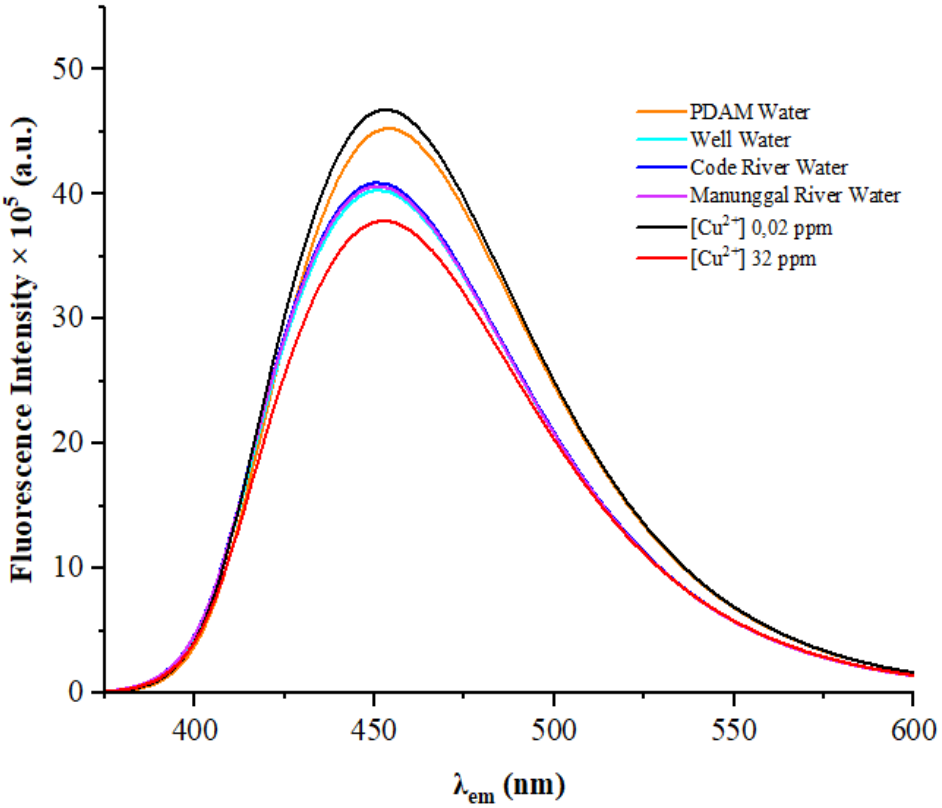

FIGURE 13. Fluorescence spectra of N,P-CDs after the addition of various real samples

TABLE 1. Analysis of Cu^{2+} in several types of water samples by using fluorescent sensor

Samples	%quenching	[Cu^{2+}/ppm]	%RSD (n=4)
PDAM water	9.0339	0.50	0.18
Well water	19.0493	1.06	0.19
Code River water	17.8124	0.99	0.27
Manunggal River water	18.3664	1.03	0.65

CONCLUSION

In this study, N, P-doped carbon dots (N,P-CDs) were successfully synthesized under optimal conditions, utilizing 25% nitrogen and 25% phosphorus dopants, via microwave irradiation at 450 W for 1.5 min. The resulting N,P-CDs exhibited enhanced fluorescence and a quasi-spherical morphology with an average size of 1.70 nm. The probe demonstrated high selectivity and sensitivity for Cu^{2+} detection, with a significant fluorescence quenching response attributed to the photoinduced electron transfer (PET) mechanism. The low LOD (0.0177 ppm) and LOQ (0.0592 ppm) values indicate that the sensor is suitable for environmental monitoring, with detection limits that are below the WHO standards. Furthermore, successful application of the N,P-CDs sensor in real water samples such as PDAM water, well water, and river water with %RSD values below 5% confirmed its potential as reliable, sensitive, and cost-effective tools for routine Cu^{2+} ions detection in aquatic environments.

ACKNOWLEDGEMENTS

We would like to thank the Ministry of Higher Education, Science and Technology of Republic Indonesia for supporting this activity through Magister Thesis Research scheme with the contract number: 067/C3.DT.05.00/PL/2025 and 2611/UN1/DITLIT/Dit-Lit/PT.01.03/2025. 067/C3/DT.05.00/PL/2025 and 2611/UN1/DITLIT/Dit-Lit/PT.01.03/2025. We also confirm that there are no conflicts of interest to declare.

REFERENCES

Al Farsi, B., Sofin, R.G.S., Al Shidhani, H., El-Shafey, E.I., Al-Hosni, A.S., Al Marzouqi, F., Issac, A., Al Nabhani, A. & Abou-Zied, O.K. 2022. The effect of microwave power level and post-synthesis annealing treatment on oxygen-based functional groups present on carbon quantum dots. *Journal of Luminescence* 252: 119326.

Algethami, F.K. & Abdelhamid, H.N. 2024. Heteroatoms-doped carbon dots as dual probes for heavy metal detection. *Talanta* 273: 125893.

Alkian, I., Sutanto, H. & Hadiyanto. 2022. Quantum yield optimization of carbon dots using response surface methodology and its application as control of Fe^{3+} ion levels in drinking water. *Material Research Express* 9: 015702.

Atchudan, R., Edison, T.N.J.I., Perumal, S., Muthuchamy, N. & Lee, Y.R. 2020. Hydrophilic nitrogen-doped carbon dots from biowaste using dwarf banana peel for environmental and biological applications. *Fuel* 275: 117821.

Brito, T.A., Costa, F.S., Oliveira, R.C., Amaral, C.D.B., Labuto, G. & Gonzalez, M.H. 2025. Green extraction using natural deep eutectic solvents for determination of As, Cd, and Pb in plant and food matrices by ICP-MS. *Food Chemistry* 464(Part 3): 141922.

Diana, F.R.M., Suratman, A., Wahyuni, E.T., Mudasir, M. & Suherman, S. 2022. Development of N,S-CDs fluorescent probe method for early detection of cr(VI) in the environment. *Chemistry Paper* 76(12): 7793-7809.

Erdiwansyah, Gani, A., Desvita, H., Mahidin, Bahagia, Mamat, R. & Rosdi, S.M. 2025. Investigation of heavy metal concentrations for biocoke by using ICP-OES. *Results in Engineering* 25: 103717.

Fu, Q., Sun, S., Lu, K., Li, N. & Dong, Z. 2024. Boron-doped carbon dots: Doping strategies, performance effects, and applications. *Chinese Chemical Letters* 35(7): 109136.

Gong, X., Li, Z., Hu, Q., Zhou, R., Shuang, S. & Dong, C. 2017. N,S,P Co-doped carbon nanodot fabricated from waste microorganism and its application for label-free recognition of manganese(VII) and L-ascorbic acid and and logic gate operation. *Applied Materials Interfaces* 9: 38761-38772.

Huang, S., Yang, E., Liu, Y., Yao, J., Su, W. & Xiao, Q. 2018. Low-temperature rapid synthesis of nitrogen and phosphorus dual-doped carbon dots for multicolor cellular imaging and hemoglobin probing in human blood. *Sensors and Actuators B: Chemical* 265: 326-334.

Issa, M.A., Abidin, Z.Z., Sobri, S., Rashid, S., Mahdi, M.A., Ibrahim, N.A. & Pudza, M.Y. 2019. Facile synthesis of nitrogen-doped carbon dots from lignocellulosic waste. *Nanomaterials* 9(10): 1500.

Kamal, A.H., Kannouma, R.E., Hammad, M.A. & Mansour, F.R. 2024. Rapid microwave fabrication of highly luminescent nitrogen and phosphorous co-doped carbon quantum dots for the determination of glutathione in pharmaceutical supplements. *Microchemical Journal* 206: 111488.

Kaur, J., Sharma, S., Mehta, S.K. & Kansal, S.K. 2020. Highly photoluminescent and pH sensitive nitrogen doped carbon dots (NCDs) as a fluorescent sensor for the efficient detection of Cr (VI) ions in aqueous media. *Spectrochimica Acta Part A: Molecular and Biomolecular Spectrosc*opy 227: 117572.

Lin, L., Wang, Y., Xiao, Y. & Liu, W. 2019. Hydrothermal synthesis of carbon dots codoped with nitrogen and phosphorus as a turn-on fluorescent probe for cadmium(II). *Microchimica Acta* 186: 147.

Liu, C., Zhang, F., Hu, J., Gao, W. & Zhang, M. 2021. A mini review on pH sensitive photoluminescence in carbon nanodots. *Frontier in Chemistry* 8: 605028.

Liu, C., Tang, B., Zhang, S., Zhou, M., Yang, M., Liu, Y., Zhang, Z.L., Zhang, B. & Pang, D.W. 2018. Photoinduced electron transfer mediated by coordination between carboxyl on carbon nanodots and Cu^{2+} quenching photoluminescence. *The Journal of Physical Chemistry* 122(6): 3662-3668.

Lou, Z., Zhou, X., Hao, X., Yang, F., Zhang, W., Feng, X., Yu, H., Cui, J., Gao, J., Xiong, Y. & Lian, Y. 2025. Ultrasensitive and selective nitrogen-doped fluorescent carbon dots probe for quantification analysis of trace Cu^{2+} in the aqueous environment. *Journal of Fluorescence* 35: 8155-8166.

Park, J., You, I., Shin, S. & Jeong, U. 2015. Material approaches to stretchable strain sensors. *Chemical Physical Chemistry* 16: 1155-1163.

Sahu, V. & Khan, F. 2020. Synthesis of bovine serum albumin capped boron-doped carbon dots for sensitive and selective detection of pb(II) ion. *Heliyon* 6(5): e03957.

Shen, Y., Wu, H., Li, J., Liu, G., Xiao, Y., Dai, Z. & Zhen, H. 2021. One-step hydrothermal method for preparing carbon dots and its determination of lead (II). *Journal of Physic: Conference Series* 2011: 012101.

Shi, Y., Zhang, W., Xue, Y. & Zhang, J. 2023. Fluorescent sensors for detecting and imaging metal ions in biological systems: Recent advances and future perspectives. *Chemosensors* 11(4): 226.

Suaad Hadi Hassan Al-Taai. 2021. Water pollution its causes and effects. *IOP Conference Series: Earth Environmental Science* 790: 012026.

Sutanto, H., Alkian, I., Romanda, N., Lewa, I.W.L., Marhaendrajaya, I. & Triadyaksa, P. 2020. High green-emission carbon dots and its optical properties: Microwave power effect. *AIP Advances* 10: 055008.

Tabaraki, R. & Abdi, O. 2020. Fluorescent sensing of Pb^{2+} by microwave-assisted synthesized N-doped carbon dots: Application of response surface methodology and Doehlert design. *Journal of the Iranian Chemical Society* 17: 839-846.

Tan, D., Zhou, S., Shimotsuma, Y., Miura, K. & Qiu, J. 2014. Effect of UV irradiation on photoluminescence of carbon dots. *Optical Materials Express* 4(2): 213-219.

Wang, X., Lin, W., Chen, C., Kong, L., Huang, Z., Kirsanov, D., Legin, A., Wan, H. & Wang, P. 2022. Neural networks based fluorescence and electrochemistry dual-modal sensor for sensitive and precise detection of cadmium and lead simultaneously. *Sensor & Actuators B: Chemical* 366: 131922.

Yan, F., Sun, Z., Zhang, H., Sun, X., Jiang, Y. & Bai, Z. 2019. The fluorescence mechanism of carbon dots, and methods for tuning their emission color: A review. *Microchimica Acta* 186: 583.

Yang, X., Zhang, Y., Liu, W., Gao, J. & Zheng, Y. 2019. Confined synthesis of phosphorus, nitrogen co-doped carbon dots with green luminescence and anion recognition performance. *Polyhedron* 171: 389-395.

Zhang, L., Wang, H., Hu, Q., Guo, X., Li, L., Shuang, S., Gong, X. & Dong, C. 2019. Carbon quantum dots doped with phosphorus and nitrogen are a viable fluorescent nanoprobe for determination and cellular imaging of vitamin B12 and cobalt(II). *Microchimica Acta* 186: 506.

Zhang, Q., He, S., Zheng, K., Zhang, L., Lin, L., Chen, F., Du, X. & Li, B. 2022. Green synthesis of mustard seeds carbon dots and study on fluorescence quenching mechanism of Fe^{3+} ions. *Inorganic Chemistry Communications* 146: 110034.

Zhang, Y., Wang, Y., Feng, X., Zhang, F., Yang, Y. & Liu, X. 2016. Effect of reaction temperature on structure and fluorescence properties of nitrogen-doped carbon dots. *Applied Surface Science* 387: 1236-1246.

Zhou, J., Zhou, H., Tang, J., Deng, S., Yan, F., Li, W. & Qu, M. 2017. Carbon dots doped with heteroatoms for fluorescent bioimaging: A review. *Microchimica Acta* 184: 343-368.

*Corresponding author; email: suherman.mipa@ugm.ac.id